IEEE Open Access Journal of
Power and Energy

Received 14 March 2021; revised 15 June 2021; accepted 7 July 2021.
Date of publication 13 July 2021; date of current version 9 November 2021.

Digital Object Identifier 10.1109/OAJPE.2021.3096811

Load Factor Assessment of the Electric Grid by the Optimal Scheduling of Electrical Equipment- A MIQCP Model

FERNANDO V. CERNA[1] (Member, IEEE), MAHDI POURAKBARI-KASMAEI[2] (Senior Member, IEEE), EHSAN NADERI[3] (Graduate Student Member, IEEE), MATTI LEHTONEN[2], AND JAVIER CONTRERAS[4] (Fellow, IEEE)

[1]Department of Electrical Engineering, Federal University of Roraima, Boa Vista, Roraima 69310-000, Brazil
[2]Department of Electrical Engineering and Automation, Aalto University, 02150 Espoo, Finland
[3]School of Electrical, Computer, and Biomedical Engineering, Southern Illinois University, Carbondale, IL 62901, USA
[4]E.T.S. de Ingeniería Industrial, University of Castilla–La Mancha, 13071 Ciudad Real, Spain

CORRESPONDING AUTHOR: J. CONTRERAS (javier.contreras@uclm.es)

This work was supported in part by the Ministry of Science, Innovation and Universities of Spain under Project RTI2018-096108-A-I00 and Project RTI2018-098703-B-I00 (MCIU/AEI/FEDER, UE) and in part by the Universidad de Castilla-La Mancha under Grant 2021-GRIN-30952.

ABSTRACT In recent years, demand-side management (DSM) strategies have become an indispensable tool in the operation and planning of modern electricity grids (EGs). One effective way of ensuring the economical and reliable operation of an EG is through assessing its load factor (LF), while considering different types of electrical equipment (e.g., residential, commercial, and industrial). Toward this end, this paper proposes a mixed-integer quadratically constrained programming (MIQCP) model to deal with the LF assessment problems in a modified power distribution system through optimal scheduling of electrical equipment. This MIQCP model aims to minimize the total costs of purchasing energy by the electric utility via an iterative process, in which the difference between the energy consumption in each period and the average consumption is reduced. In the proposed model, the uncertainties in the consumption habits of different consumers, information related to each electrical equipment, energy prices, and the grid's technical constraints are considered. A modified 34-node EG, differentiated by consumer type, is implemented to evaluate the proposed model. Results show that the LF value is related to the optimal scheme of the electrical equipment that meets the operational and economic requirements of the power grid.

INDEX TERMS Demand-side management, electricity grid, electrical equipment, load factor, MIQCP model.

NOMENCLATURE

A. SETS AND INDEXES

B	Set of nodes i.
$\mathcal{K}$	Set of electrical equipment types k.
$\mathcal{L}$	Set of branches ij.
$\mathcal{T}$	Set of periods t.
i	Indexes for nodes.
ij	Indexes for branches.
k	Indexes standing for electrical equipment.
s	Indexes standing for consumer units.
t	Indexes standing for periods.

B. PARAMETERS

$\|.\|$	Cardinal of set.
α	Step value in each iteration.
δ_t	Energy price at period t (\$/kWh).
ζ	Parameter assuming the value of t in which an electrical equipment will be used.
θ	Random value ranging from 0 to 100.
λ_k	Binary parameter indicating whether electrical equipment of type k will be controlled as part of the DSM program.
ξ	Accumulator.
$\pi^{hc}_{i,k,t}$	Habitual consumption at period t of electrical equipment of type k belonging to node i (kWh).
$\bar{\Gamma}_e$	Upper limit of the difference between average consumption and consumption per period.
Γ^0	Maximum positive value obtained from the difference of ψ_t and ψ^{lp}.

$\bar{\Delta}^s_{ij}$ Upper limit of discretization blocks.
Δt Duration of each period of usage (h).
$D^u_{k,t}$ Percentage value indicating the probability of usage of electrical equipment of type k at period t.
$D^n_{k,t}$ Parameter associated with the normalized values of $D^u_{k,t}$.
$D^a_{k,t}$ Accumulated distribution related to the values of $D^n_{k,t}$.
e Iteration counter.
h_k Number of usage periods of electrical equipment of type k (h).
$H^b_{i,s,k,t}$ Binary matrix indicating, at period t, the state of usage of electrical equipment of type k at node i of consumer unit s ($s \in 1, \ldots, n^u_i$).
$H^c_{i,s,k,t}$ Continuous matrix indicating, at period t, the demand from the usage of electrical equipment of type k at node i of consumer unit s ($s \in 1, \ldots, n^u_i$) (kW).
$\underline{I}_{ij}, \overline{I}_{ij}$ Lower and upper limits of current flowing into branch ij (A).
m_k Indicates, for period t, the number of periods backward or forward in which electrical equipment of type k can be initially connected.
$m^s_{ij,y}$ Slope of the y$^{\text{th}}$ block associated with the branch ij.
n^{iter} Predefined number of iterations.
n^u_i Number of users associated with node i.
$N_{k,t}$ Number of units of electrical equipment of type k connected at period t.
$P^{eu}_{k,t}$ Average power of electrical equipment of type k at period t (kW).
r_{ij} Resistance of branch ij (kΩ).
t^b_i Type of node i (0: for load and transfer, and 1: substation).
t^l_i Type of load connected at node i (1: residential, 2: commercial, and 3: industrial).
V Nominal voltage value (kV).
$\underline{V}, \overline{V}$ Lower and upper limit of voltage magnitude (kV).
x_{ij} Reactance of branch ij (kΩ).
Y Number of discretization blocks.
z_{ij} Impedance of branch ij (kΩ).

C. VARIABLES

ψ_t Energy consumption by all consumers at period t (kWh).
$\overline{\psi}$ Maximum value of ψ_t (kWh).
ψ^{av}_t Average value of the energy consumed by all consumers at period t (kWh).
ψ^{lp} Average value of the energy consumed by all consumers in the last period of a day (kWh).
$\Pi^{conn}_{i,k,t}$ Energy consumption by electrical equipment of type k connected at period t belonging to node i (kWh).
$\Pi^{dconn}_{i,k,t}$ Energy consumption by electrical equipment of type k disconnected at period t belonging to node i (kWh).
$\Pi^{oc}_{i,k,t}$ Optimal consumption at period t of electrical equipment of type k at node i (kWh).
$\Delta\Pi_{i,k,t}$ Difference between $\Pi^{conn}_{i,k,t}$ and $\Pi^{dconn}_{i,k,t}$.
$\Delta^p_{ij,t,y}$ Value of the y^{th} block of $P_{ij,t}$.
$\Delta^q_{ij,t,y}$ Value of the y^{th} block of $Q_{ij,t}$.
$I^{sqr}_{ij,t}$ Square of the current magnitude of branch ij at period t (A).
$n_{i,k,u,v}$ Number of units of electrical equipment of type k belonging to node i to be shifted from period u to v.
$P^d_{i,t}$ Active power demand in node i at period t (kW).
$P^s_{i,t}$ Active power provided by substation in node i at period t (kW).
$P_{ij,t}$ Active power flow of branch ij at period t (kW).
$p^+_{ij,t}$ Auxiliary variable related to $P_{ij,t}$.
$p^-_{ij,t}$ Auxiliary variable related to $P_{ij,t}$.
$Q^d_{i,t}$ Reactive power demand in node i at period t (kvar).
$Q^s_{i,t}$ Reactive power provided by substation in node i at period t (kvar).
$Q_{ij,t}$ Reactive power flow of branch ij at period t (kvar).
$q^+_{ij,t}$ Auxiliary variable related to $Q_{ij,t}$.
$q^-_{ij,t}$ Auxiliary variable related to $Q_{ij,t}$.
$V^{sqr}_{i,t}$ Square of the voltage magnitude of node i at period t (kV).

I. INTRODUCTION

A. CONTEXT

DEMAND-SIDE management (DSM) strategies reinforcing the link between energy cost saving in consumption sectors and the reliability of the electricity grid (EG) are effective tools in the normal operation of modern-day power systems [1]. To meet the energy requirements of various kinds of consumers (e.g., residential, commercial, and industrial, as the most conspicuous ones) in a typical EG, information associated with consumption patterns in the aforementioned sectors needs to be updated expeditiously in the electric utility database [2]. To this end, the role of metering and communications infrastructure is used for the continuous and reliable transfer of bidirectional information flow between the data center and the smart meter located in each consumer unit [3]. Consumer units participating in DSM programs can achieve energy cost savings through efficient scheduling of their electrical equipment for day-ahead, this scheduling being driven by tariff signals, e.g., TOU, RTP, etc. [4]. In this way, the energy consumption at the peak period is reduced and/or shifted to off-peak periods; thus, the DSM program is able to reshape the consumption profile of each class of consumers as well as the total demand

profile. Several optimization targets that include the scheduling of the electrical equipment used in different activities or processes within the consumer classes can be defined. However, in this research, the main target is to improve the load factor (LF) of a modified EG with different types of consumers, as pointed out earlier. The LF is defined as the ratio between average demand and maximum demand for a given period (e.g., day, week, etc.) [5]. The LF value represents the level of reshaping the consumption profile obtained through the reduction of peak demand or by an increase in energy usage at periods corresponding to the valleys in consumption profile [6]. The LF value ranges from 0 to 1; therefore, when LF is close to its maximum value, 1, the consumption profile shows i) reduction in peak demand and ii) redistribution of demand throughout the day, otherwise, there are periods of the day with high peak demand, causing economic losses in the EG operation [7]. As a result, the full potential of DSM strategies can be achieved via assessing the LF as part of the energy supply to different consumer types in an EG [8]. In addition, operational limits related to the EG, such as current capacity of the feeders, active power losses, voltage profile, as well as voltage drop values of the main feeders, should also be taken into account when determining the LF value [9]. Therefore, to harness the aforementioned issues, this work aims to develop an optimization tool allowing evaluation of LF associated with a modified EG through suitable DSM strategies, while a set of technical constraints needs to be considered for the power flow, and the electrical equipment usage patterns.

B. RELATED WORKS

A literature survey shows that the importance of the LF value in evaluating the operation of an EG has recently been studied in different works. As an illustration, in [10], an algorithm based on neural networks was used to forecast the annual demand profile of an EG with low LF. In [11], the LF value of an EG was increased through the reconfiguration of a set of feeders, called distribution feeder reconfiguration (DFR). An analysis associated with the performance of a set of EGs that were differentiated by their LF values was presented in [12], in which, in each case, minimizing the cost of energy losses had a significant impact on the LF. A load controller (LC) considering the scheduling of heating loads in a given node of an EG was developed in [13]. The LF evaluation at this given node was performed by the LC, considering the voltage levels. The LF improvement related to an industrial plant and also the EG of the University of North East India was addressed in [5] and [14], respectively. In this regard, in [5], a technique based on direct control was used, whereas, in [14], an increase of LF value was obtained via the efficient management of active power losses in feeders. In [15], the improvement of the LF of an EG was achieved by reducing the number of EV batteries to be charged during peak hours. An evolutionary algorithm was developed in [16] to coordinate the power flow in distribution systems with adjustable LF. In [17], DSM techniques were applied to a sustainable building in order to improve the LF. In [18], a multi-objective algorithm was developed, aiming to minimize the energy consumption costs as well as maximize the LF of the residential grid. The aforementioned works address the improvement of the LF considering the reduction in peak demand due to the presence of renewable sources and EVs in the EG. However, the constraints related to voltage variation, power balance, active losses, were not explicitly found in these studies. Regarding DSM, there are several works in literature investigating the effects of DSM programs while neglecting the importance of the LF. Thus, in [19], [20], DSM strategies based on the stochastic pricing structure, RES integration, as well as real-time information, were implemented aiming at reducing carbon emissions. Using a multi-objective optimization model, [21] analyzed the benefits of DSM programs on the generation side, mainly in reducing the production costs of thermal plants. Participation of energy storage systems (ESSs), as supporting devices for demand management during the day, was investigated in [22]. A stochastic quadratic programming model (SQPM) was developed in [23] to reduce the consumption of electrical loads in an industrial unit during the day. The impact of DSM actions on a 295-node power grid was analyzed in [24]. In [25], [26], DSM techniques based on game theory were developed to reduce the fuel waste and contaminants emitted by the energy generation sector as well as the peak demand from users. A DSM strategy based on three hierarchies, namely i) electric utility, ii) demand response aggregator, and iii) consumers was proposed in [27] to minimize the total cost associated with system operation, while the benefits of the aggregator were guaranteed. Despite the different approaches mentioned above, there are still gaps with regard to improving the LF while guaranteeing the economic and reliable performance of the EG. Therefore, this research tries to fill this knowledge gap in the search for mutual financial benefits for consumers and electric power companies. Table 1 highlights the advantages (✓) and disadvantages (×) of each work mentioned above in comparison with the present approach. Characteristics that are taken into account are: improvement of the LF of a group of consumers (c1); reduction of active losses and improvement of the voltage profile in the EG (c2); mitigation of the occurrence of new peaks in demand (c3); and DSM of equipment types (c4).

TABLE 1. Analysis of related works.

References	Features			
	c1	c2	c3	c4
[5], [10], [12], [15]-[16]	✓	×	×	×
[11]	✓	✓	×	×
[13]	✓	×	×	✓
[14]	✓	✓	×	×
[17]-[18]	✓	×	×	✓
[19], [20]-[23], [25]-[27]	×	×	×	✓
[24]	×	✓	×	✓
This paper (MIQCP Model)	✓	✓	✓	✓

C. CONTRIBUTIONS

Although in almost all of the aforementioned works, DSM techniques were used to reduce costs of energy consumption expenditures, their effects on the operational performance of the EG, i.e., on voltage variation as well as on losses of active power, were neglected. In this regard, in order to improve these issues, this paper elaborates on a MIQCP model for efficient assessment of the LF over an EG through DSM strategies. The proposed model aims to minimize the total costs associated with the energy purchase by an electric utility. The model uses an iterative process for reducing the difference between the energy consumed in each period and the average consumption value of the day. Moreover, the uncertainties in the consumption patterns of the consumer units present in the EG are represented using a Monte Carlo Simulation (MCS) algorithm. Information related to each electrical equipment, and operational constraints related to voltage limits, feeder current limits, power losses, etc., during the EG operation, are considered as well. All in all, the main contributions of this paper are elaborated upon hereunder.

- Proposing computationally-efficient MIQCP model for the proper LF assessment associated with an EG using a DSM strategy.
- Analyzing the problems inherent to the EG operation, such as variation in voltage and active power losses that are a consequence of DSM programs. The proposed methodology allows power system operators to manage energy usage rationally, guaranteeing a reliable performance of the EG within its operational limits.
- Investigating the potential impact of reducing the electrical demand during peak periods, mitigating the appearance of new peaks during off-peak hours, through the large-scale shifting of electrical equipment in the residential, commercial, and industrial types of consumers.

The remaining parts of this paper are organized as follows. The hypotheses assumed, electrical equipment usage patterns, and the EG parameters are presented in Section 2. Section 3 formulates the MIQCP model, and explains the linearization process. Section 4 provides a practical case study and, finally, Section 5 provides conclusions.

II. SIMULATION SETUP

In this section, the main hypotheses related to consumer units, electrical equipment, and energy tariffs are introduced. Due to the difficulty of obtaining information related to the habitual consumption patterns for each class of consumers, an algorithm that simulates the patterns of the electrical equipment usage is implemented based on [28]. Additionally, the technical data connected with the proposed EG scheme are presented in detail.

A. HYPOTHESES

In this work, the following hypotheses are taken into consideration.

1) For each class of consumer (i.e., residential, commercial, or industrial) in the EG, a habitual consumption profile is assigned, which represents the behavior pattern of the consumer when using a given electrical equipment.
2) Consumers of the same class have an equal type number of electrical equipment k. For instance, in the case of residential consumers, all of them have an equal type number of electrical equipment.
3) In order to analyze the level of active power losses in the main feeders and adjacent cables during supply power to the consumer units, each electrical equipment is considered to be a purely resistive load with a unitary power factor (PF).
4) A probability distribution is used to represents the usage pattern of each electrical equipment throughout the day.
5) The hourly price for energy consumption has different tariff levels.

TABLE 2. Consumption data for electrical equipment.

k	Electrical equipment	$P^{eu}_{k,t}$ (kW) 1st (h)	2nd (h)	3rd (h)	4th (h)	5th (h)	6th (h)	h_k (h)
	Residential equipment							
1	Dryer	1.2	-	-	-	-	-	1
2	Dish Washer	0.7	-	-	-	-	-	1
3	Washing Machine	0.5	0.4	-	-	-	-	2
4	Oven	1.3	-	-	-	-	-	1
5	Iron	1.0	-	-	-	-	-	1
6	Vaccum Cleaner	0.4	-	-	-	-	-	1
7	Fan	0.2	0.2	0.2	-	-	-	3
8	Kettle	2.0	-	-	-	-	-	1
9	Toaster	0.9	-	-	-	-	-	1
10	Rice Cooker	0.85	-	-	-	-	-	1
11	Hair Dryer	1.5	-	-	-	-	-	1
12	Blender	0.3	-	-	-	-	-	1
13	Frying Pan	1.1	-	-	-	-	-	1
14	Coffee Maker	0.8	-	-	-	-	-	1
	Commercial equipment							
1	Water Dispenser	2.5	-	-	-	-	-	1
2	Dryer	3.5	-	-	-	-	-	1
3	Kettle	3.0	2.5	-	-	-	-	2
4	Oven	5.0	-	-	-	-	-	1
5	Coffee Maker	2.0	2.0	-	-	-	-	2
6	Fan/AC	3.5	3.0	-	-	-	-	2
7	Air Conditioner	4.0	3.5	3.0	-	-	-	3
8	Lights	2.0	1.75	1.50	-	-	-	3
	Industrial equipment							
1	Water Heater	12.5	12.5	12.5	12.5	-	-	4
2	Welding Machine	25	25	25	25	25	-	5
3	Fan/AC	30	30	30	30	30	-	5
4	Arc Furnance	50	50	50	50	50	50	6
5	Induction Motor	100	100	100	100	100	100	6
6	DC Motor	150	150	150	-	-	-	3

B. ELECTRICAL EQUIPMENT CONSUMPTION PATTERNS

Information regarding the consumption of each electrical equipment, being a residential, commercial, or industrial unit, is shown in Table 2 [29]. Taking into account the type number of electrical equipment for each residential unit and the total number of residential units, a total of 1876 electrical equipment units are found, which are used in different periods of the day, depending on the consumption pattern of each

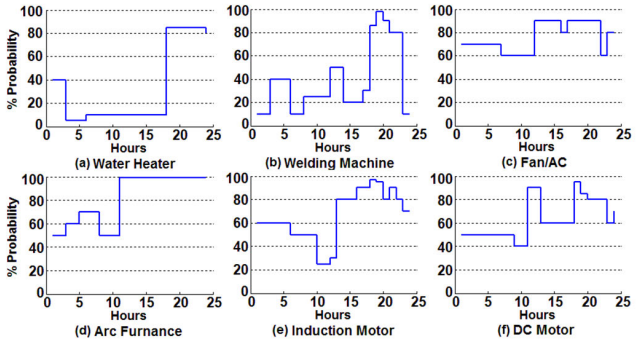

FIGURE 1. The values of consumption probability related to industrial electrical equipment.

consumer unit. Similarly, for the 39 commercial and 13 industrial units, the total number of electrical equipment units are 273 and 78, respectively.

Consumption patterns of the electrical equipment are established through a probability distribution, $D^u_{k,t}$. In this way, each equipment of type k corresponding to a given consumer unit has a set of $D^u_{k,t}$ values for the day [30]. As an illustration, the values of $D^u_{k,t}$ associated with electrical equipment presented in industrial units are shown in Fig. 1. It should be noted that these probability values are based on [31], [32] and indicate, for each period t, the probability of electric equipment being turned on (for energy consumption) during that period.

Based on the probability values depicted in Fig. 1, the MCS algorithm, shown in Fig. 2, is run to determine the consumption profile associated with the available electrical equipment in the EG [33], [34].

According to Fig. 2, the algorithm starts with the predefined values of $D^u_{k,t}$, $P^{eu}_{k,t}$, and h_k, which are the probability distribution of equipment of type k for each period t of the day, the average power, and also the number of usage periods of equipment of type k. Further, each value of $H^b_{i,s,k,t}$ and $H^c_{i,s,k,t}$ is initialized to zero. Afterward, a set of iterations corresponding to each equipment of type k at each period t are made to calculate the value of $D^n_{k,t}$. Hence, for each value of k and t, the value of $D^n_{k,t}$ is obtained when $D^u_{k,t}$ is multiplied by 100 and divided by $\sum_{\forall\tau\in\mathcal{T}} D^u_{k,\tau}$. Then, two predefined conditions, $t = |\mathcal{T}|$ and $k = |\mathcal{K}|$, are evaluated. In this regard, when both conditions are met, the iterations for k and t end; otherwise, the calculation of $D^n_{k,t}$ continues.

Another iterative process, which is related to t and k, is performed to calculate the values of $D^a_{k,t}$ taking into account the values of $D^n_{k,t}$ obtained in the previous steps. Thus, for all equipment of type k, the accumulator value ξ is set to zero. Consequently, in each iteration t, the values of $D^n_{k,t}$ are accumulated in ξ to immediately be assigned to $D^a_{k,t}$.

The cumulative probability values, $D^a_{k,t}$, are used to establish the period t of the day when the equipment of type k is turned on for energy consumption. For this purpose, another iterative process is performed for each node i in each consumer unit s, and for each equipment of type k, where a random number θ is generated before executing the iteration associated with the set of periods t. Next, in each iteration of set $\mathcal{T}$, the value of t is compared under the predefined condition $t > 1$. If the aforementioned condition is not met, the generated value of θ is compared under a new condition, $0 \le \theta \le D^a_{k,t}$, otherwise, the condition of $D^a_{k,t-1} \le \theta \le D^a_{k,t}$ is checked. If either of these conditions is met, a unit value is assigned to $H^b_{i,s,k,t}$.

After that, the conditions of $t = |\mathcal{T}|$, $k = |\mathcal{K}|$, $s = \left|1 \ldots n^u_k\right|$, and $i = |\mathcal{B}|$ are sequentially evaluated. The iterative process for t, k, s, and i is terminated as soon as each of these conditions is met; otherwise, the assignment of unit values for $H^b_{i,s,k,t}$ continues to be computed. Now, the $N_{k,t}$ values are calculated within the iterative process associated with each equipment type k each period t. Note that these values are computed considering the unit values of $H^b_{i,s,k,t}$. The values of $H^c_{i,s,k,t}$ are determined within another set of iterations. In this set, each iterative process is done considering each value of t, k, s, and i. Thus, each value of $H^c_{i,s,k,t}$ is obtained by the product of $P^{eu}_{k,t} \times H^b_{i,s,k,t}$. Thereafter, the conditions of $t = |\mathcal{T}|$, $k = |\mathcal{K}|$, $s = \left|1 \ldots n^u_k\right|$ and $i = |\mathcal{B}|$, are rechecked. When each of the conditions is met, the $H^c_{i,s,k,t}$ calculation process stops; otherwise, it continues.

The unit values of $H^b_{i,s,k,t}$ representing the rest of the periods of the day when electrical equipment type k is switched on for its energy consumption are determined next. As a result, iterations associated with the set of periods t are made in order to obtain from $H^b_{i,s,k,t}$ the first period t at which each equipment k was turned on. In this regard, each value of t is evaluated simultaneously under two conditions, $t \le |\mathcal{T}| - (h_k - 1)$ and $H^b_{i,s,k,t} = 1$. If both aforementioned conditions are satisfied, the value of t is assigned to ζ, and, then, condition $t = |\mathcal{T}|$ is checked; otherwise, only the condition $t = |\mathcal{T}|$ is checked. When the latter condition is not satisfied another iteration is performed.

Next, the new iterative process related to t is terminated, and the condition of $t = \zeta$ is evaluated. If the condition is not met, $H^b_{i,s,k,t}$ adopts the value zero, then the condition of $t = |\mathcal{T}|$ needs to be checked; otherwise, another iterative process for t' is performed.

In the iterative process, when the condition of $t' > t$ is satisfied, a unit value is assigned to $H^b_{i,s,k,t'}$, and then $H^c_{i,s,k,t'}$ is calculated as $P^{eu}_{k,t'} \times H^b_{i,s,k,t'}$; otherwise, another iteration t' is performed. After the calculation of $H^c_{i,s,k,t'}$, the condition of $\sum_{\forall\tau\in\mathcal{T}} H^b_{i,s,k,\tau} = h_k$ is evaluated. If this condition is not met, another iteration t' is executed; otherwise, each condition $i = |\mathcal{B}|$, $s = \left|1, \ldots, n^u_i\right|$, $k = |\mathcal{K}|$, and $t = |\mathcal{T}|$ is evaluated until each process ends.

Finally, a last iterative process for values of i, k, and t is performed in order to calculate $\pi^{hc}_{i,k,t}$. Note that the $\pi^{hc}_{i,k,t}$ values for each i, k, and t are obtained as the sum of all $H^c_{i,s,k,t}$ values for s from 1 to n^u_i. This calculation is ceased when the conditions of $i = |\mathcal{B}|$, $k = |\mathcal{K}|$, and $t = |\mathcal{T}|$ are completely satisfied.

As a result of running the MCS algorithm, the habitual consumption profile $\pi^{hc}_{i,k,t}$ is obtained. This profile represents,

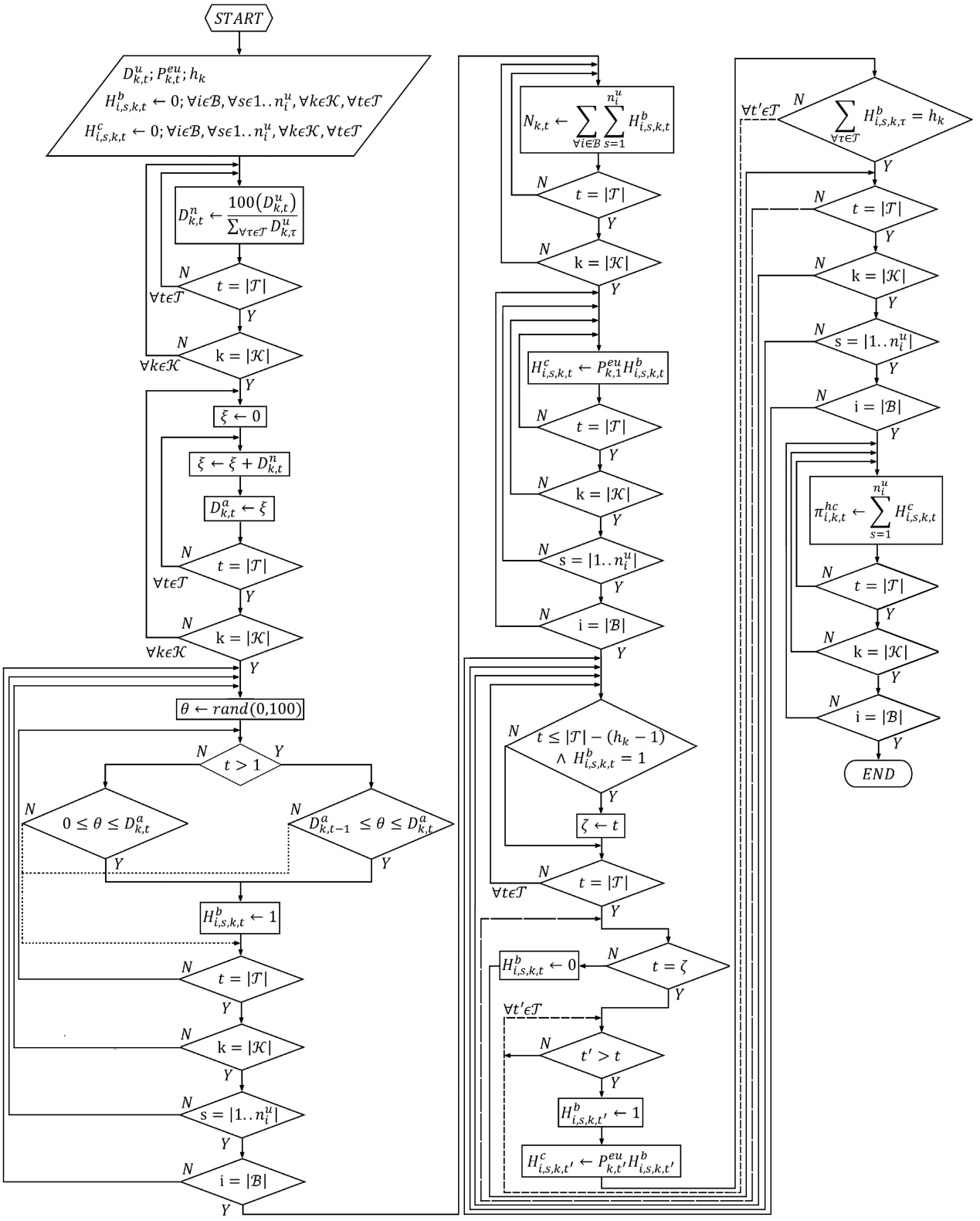

FIGURE 2. **MCS algorithm.**

for period t, the energy consumption of all equipment k at node i. It is worth mentioning that $\pi^{hc}_{i,k,t}$ simulates the habitual consumption patterns of consumer units at a given node i. In addition, $\pi^{hc}_{i,k,t}$ is constructed based on the probability distribution values $D^u_{k,t}$ for each type of equipment k, as well as the information in Table 2. Once $\pi^{hc}_{i,k,t}$ is determined,

the MIQCP model uses it as input information to build the optimal $\Pi^{oc}_{i,k,t}$ profile. In the mathematical formulation of the proposed model, detailed in Section III, $\pi^{hc}_{i,k,t}$ is presented in constraints (2) and (8). Through both constraints, the MIQCP model seeks to determine the $\Pi^{oc}_{i,k,t}$ profile with the best LF and without the presence of new consumption peaks that exceed the highest $\pi^{hc}_{i,k,t}$ consumption peak.

III. PROPOSED MODEL

In this section, the mathematical formulation of the proposed MIQCP model is presented in (1)–(19).

A. OBJECTIVE FUNCTION

$$\text{Min}: \sum_{\forall t\in\mathcal{T}}\sum_{\forall i\in\mathcal{B}}\sum_{\forall k\in\mathcal{K}}(\Pi^{oc}_{i,k,t}\delta_t) + \sum_{\forall t\in\mathcal{T}}\sum_{\forall ij\in\mathcal{L}}(r_{ij}I^{sqr}_{ij,t}\Delta t\delta_t) \quad (1)$$

In (1), the total cost of purchasing the energy, is shown which comprises two terms. The first term indicates the energy consumption of each consumer unit. The remaining part represents active power losses, $r_{ij}\times I^{sqr}_{ij,t}$, during the EG operation. This objective function is minimized subject to the following techno-economic constraints and limitations.

B. CONSTRAINTS

Constraints related to the proposed model are formulated as follows.

$$\Pi^{oc}_{i,k,t} = \pi^{hc}_{i,k,t} + \Delta\Pi_{i,k,t}; \forall i\in\mathcal{B}, \forall k\in\mathcal{K}, \forall t\in\mathcal{T} \quad (2)$$

$$\Delta\Pi_{i,k,t} = 0; \forall i\in\mathcal{B}, \forall k\in\mathcal{K}, \forall t\in\mathcal{T}: \lambda_k = 0 \quad (3)$$

$$\Delta\Pi_{i,k,t} = \Pi^{conn}_{i,k,t} - \Pi^{dconn}_{i,k,t}; \quad \forall i\in\mathcal{B}, \forall k\in\mathcal{K}, \forall t\in\mathcal{T}: \lambda_k = 1 \quad (4)$$

$$\Pi^{conn}_{i,k,t} = \sum_{t'=1}^{h_k}\sum_{\substack{u=1\\ :u\neq t+1-t'\wedge\\ \begin{pmatrix} u\geq t+1-t'-m_k\\ \wedge\\ u\leq t+1-t'+m_k\end{pmatrix}}}^{|\mathcal{T}|}\left(n_{i,k,u,t+1-t'}\times P^{eu}_{k,t'}\times\Delta t\right)$$
$$\forall i\in\mathcal{B}, \forall k\in\mathcal{K}, \forall t\in\mathcal{T}: \lambda_k = 1 \quad (5)$$

$$\Pi^{dconn}_{i,k,t} = \sum_{t'=1}^{h_k}\sum_{\substack{v=1\\ :v\neq t+1-t'\wedge\\ \begin{pmatrix} v\geq t+1-t'-m_k\\ \wedge\\ v\leq t+1-t'+m_k\end{pmatrix}}}^{|\mathcal{T}|+t'-h_k}\left(n_{i,k,t+1-t',v}\times P^{eu}_{k,t'}\times\Delta t\right)$$
$$\forall i\in\mathcal{B}, \forall k\in\mathcal{K}, \forall t\in\mathcal{T}: \lambda_k = 1 \quad (6)$$

$$\sum_{\forall i\in\mathcal{B}}\sum_{\substack{v=1\\ :v\neq t\wedge\\ \begin{pmatrix} v\geq t-m_k\\ \wedge\\ v\leq t+m_k\end{pmatrix}}}^{|\mathcal{T}|+1-h_k} n_{i,k,t,v} \leq N_{k,t}; \forall k\in\mathcal{K}, \forall t\in\mathcal{T}: \lambda_k = 1 \quad (7)$$

$$\sum_{\forall i\in\mathcal{B}}\sum_{\forall k\in\mathcal{K}}\Pi^{oc}_{i,k,t} \leq Max_{\forall\tau\in\mathcal{T}}\left\{\sum_{\forall i\in\mathcal{B}}\sum_{\forall k\in\mathcal{K}}\pi^{hc}_{i,k,\tau}\right\}; \forall t\in\mathcal{T} \quad (8)$$

$$\psi_t = \sum_{\forall i\in\mathcal{B}}\sum_{\forall k\in\mathcal{K}}\Pi^{oc}_{i,k,t}; \forall t\in\mathcal{T} \quad (9)$$

$$\psi^{av}_t = \frac{1}{t}\sum_{\substack{\forall\tau\in\mathcal{T}\\ :\tau\leq t}}\psi_\tau; \forall t\in\mathcal{T} \quad (10)$$

$$\psi^{lp} = \psi^{av}_t; \forall t\in\mathcal{T}: t = |\mathcal{T}| \quad (11)$$

$$\left(\psi_t - \psi^{lp}\right)^2 \leq \left(\bar{\Gamma}\right)^2; \forall t\in\mathcal{T} \quad (12)$$

$$P^d_{i,t} = \frac{1}{\Delta t}\sum_{\forall k\in\mathcal{K}}\Pi^{oc}_{i,k,t}; \forall i\in\mathcal{B}, \forall t\in\mathcal{T} \quad (13)$$

$$\sum_{\forall ki\in\mathcal{L}}P_{ki,t} - \sum_{\forall ij\in\mathcal{L}}\left(P_{ij,t} + r_{ij}\times I^{sqr}_{ij,t}\right) + P^s_{i,t} = P^d_{i,t}; \quad \forall i\in\mathcal{B}, \forall t\in\mathcal{T} \quad (14)$$

$$\sum_{\forall ki\in\mathcal{L}}Q_{ki,t} - \sum_{\forall ij\in\mathcal{L}}\left(Q_{ij,t} + x_{ij}\times I^{sqr}_{ij,t}\right) + Q^s_{i,t} = Q^d_{i,t}; \quad \forall i\in\mathcal{B}, \forall t\in\mathcal{T} \quad (15)$$

$$\mathrm{V}^{sqr}_{i,t} - 2\left(r_{ij}\times P_{ij,t} + x_{ij}\times Q_{ij,t}\right) - z^2_{ij}\times I^{sqr}_{ij,t} - \mathrm{V}^{sqr}_{j,t} = 0; \quad \forall ij\in\mathcal{L}, \forall t\in\mathcal{T} \quad (16)$$

$$V^{sqr}_{i,t}\times I^{sqr}_{ij,t} = P^2_{ij,t} + Q^2_{ij,t}; \forall ij\in\mathcal{L}, \forall t\in\mathcal{T} \quad (17)$$

$$\underline{I}^2_{ij} \leq I^{sqr}_{ij,t} \leq \bar{I}^2_{ij}; \forall ij\in\mathcal{L}, \forall t\in\mathcal{T} \quad (18)$$

$$\underline{V}^2 \leq V^{sqr}_{i,t} \leq \overline{V}^2; \forall i\in\mathcal{B}, \forall t\in\mathcal{T} \quad (19)$$

In constraints (2)–(7), the optimal profile associated with the total consumption of the consumer units is calculated by shifting consumption periods t of each electrical equipment k. In (2), the total consumption, $\Pi^{oc}_{i,k,t}$, is obtained as the sum of $\pi^{hc}_{i,k,t}$ and $\Delta\Pi_{i,k,t}$ for each node i, each equipment of type k, and at each period t. The value of $\Delta\Pi_{i,k,t}$, to be calculated only for electrical equipment of type k with $\lambda_k = 1$, is guaranteed by considering (3) and (4). Thus, for the equipment of type k present at node i with $\lambda_k = 1$, $\Delta\Pi_{i,k,t}$ is defined for a given period t as the difference between the energy consumption added to period t when the equipment of type k is connected (coming from other connection periods), $\Pi^{conn}_{i,k,t}$, and the energy consumption to be deduced from period t when the equipment k is disconnected (going to other connection periods), $\Pi^{dconn}_{i,k,t}$, (4). Calculations associated with $\Pi^{conn}_{i,k,t}$ and $\Pi^{dconn}_{i,k,t}$ are made through constraints (5) and (6), respectively. The energy consumption, $\Pi^{conn}_{i,k,t}$, in a given period t due to the connection of equipment of type k coming from period u is determined in constraint (5). In (6), the energy consumption taken out from period t and shifted to period v, $\Pi^{dconn}_{i,k,t}$ is obtained. Constraint (7) ensures that the maximum number of units of equipment of type k to be connected for consumption at period t is not exceeded. The LF assessment related to the proposed EG is established via (8)–(12). In this context, in (8), the optimal consumption of all consumer units at each period t must be less than the peak of the habitual profile. This optimal consumption obtained from a given period t is assigned to ψ_t in (9). As an illustrative example, Fig. 3 depicts, for each period t, the energy consumption, ψ_t. Note

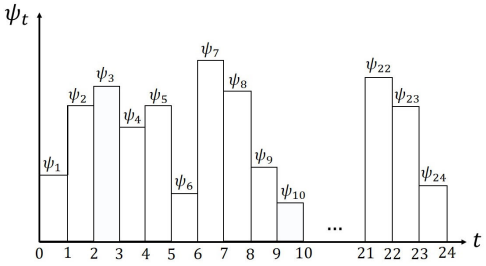

FIGURE 3. Energy consumption for each period t.

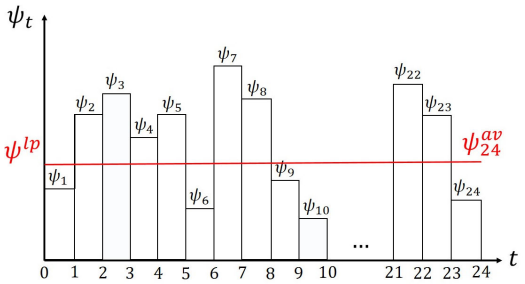

FIGURE 4. Energy consumption for each period t and the average consumption value for the day.

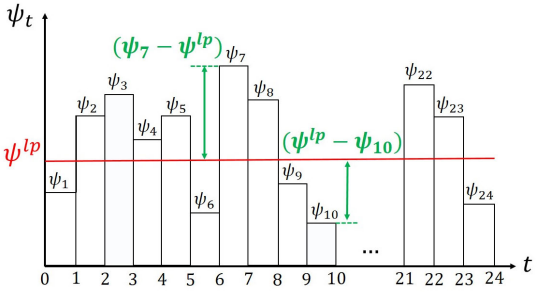

FIGURE 5. Difference between energy consumption at each period t and the average consumption value.

that for this consumption profile of the EG, the average value of energy consumption, ψ^{lp}, would be equal to $(\psi_1 + \psi_2 + \psi_3 + \ldots + \psi_{23} + \psi_{24})/24$. However, because ψ_t is a primary variable, the ψ^{lp} value cannot be calculated simultaneously. To obtain the ψ^{lp} value, (10) and (11) are used.

Using (10), the value of ψ_t^{av} at each period t is calculated. Note that this value considers the sum of the ψ_t values under the condition, $\tau \leq t$. Thus,

$$\psi_1^{av} = \frac{1}{1} \sum_{\substack{\forall \tau \in \mathcal{T} \\ :\tau \leq 1}} \psi_\tau = \frac{1}{1} (\psi_1) \,; \forall t = 1$$

$$\psi_2^{av} = \frac{1}{2} \sum_{\substack{\forall \tau \in \mathcal{T} \\ :\tau \leq 2}} \psi_\tau = \frac{1}{2} (\psi_1 + \psi_2) \,; \forall t = 2$$

$$\vdots$$

$$\psi_{23}^{av} = \frac{1}{23} \sum_{\substack{\forall \tau \in \mathcal{T} \\ :\tau \leq 23}} \psi_\tau = \frac{1}{23} (\psi_1 + \psi_2 + \psi_3 + \ldots + \psi_{23}) \,;$$

$$\forall t = 23$$

$$\psi_{24}^{av} = \frac{1}{24} \sum_{\substack{\forall \tau \in \mathcal{T} \\ :\tau \leq 24}} \psi_\tau = \frac{1}{24} (\psi_1 + \psi_2 + \psi_3 + \ldots + \psi_{23} + \psi_{24}) \,; \forall t = 24$$

Note that for $t = 24$, the value of ψ_{24}^{av} is equal to the average value of the energy consumption ψ^{lp} mentioned above. This value is necessary to schedule the types of equipment (residential, commercial and/or industrial) during the day in order to improve the LF. In this way, this value is stored through (11), once ψ_t^{av} is evaluated for t equal to $|\mathcal{T}|$, where the cardinal of the set $\mathcal{T}$ represented by $|\mathcal{T}|$, is equal to the total number of periods in a 24-hour horizon. Fig. 4 shows the value of ψ^{lp} calculated as ψ_{24}^{av}, and the consumption profile ψ_t, depicted in Fig. 3. Once the ψ^{lp} value is known, it is used in (12) to reshape the ψ_t consumption profile.

In (12), the optimal consumption profile is reshaped by the square of the difference $\psi_t - \psi^{lp}$, for each period t. In this way, the model seeks for the efficient scheduling of types of equipment that brings peak consumption close to the average consumption value. Consequently, the LF value will be increased. It is worth mentioning that the use of the square, on both sides of the inequality, aims to consider only the numerical value of $\psi_t - \psi^{lp}$ since this difference can be positive or negative, as shown by the respective cases $t = 7$, $(\psi_7 - \psi^{lp})$; and $t = 10$, $(\psi^{lp} - \psi_{10})$ shown in Fig. 5.

Finally, constraints (13)–(19) are associated with the operation of the EG [35]. In this regard, in (13), the demand $P_{i,t}^d$ for each node i at each period t is obtained considering the optimal consumption of $\Pi_{i,k,t}^{oc}$. The equilibrium of active and reactive power in the EG is represented by (14) and (15), respectively. In (16), the voltage drop is calculated for each branch ij at each period t. The relationship between active and reactive power flows and the voltage and current magnitudes is established via (17). In (18) and (19), the upper and lower limits related to the voltage and current magnitudes are guaranteed, respectively.

C. LINEARIZATION PROCESS

In the MIQCP model, constraints (12) and (17) are with nonlinear terms. In (12), given that $\overline{\Gamma}$ is a parameter, the nonlinear term corresponds to the expression on the left side $\left(\psi_t - \psi^{lp}\right)^2$. In this approach, the linearization of this term is not being performed because it participates in the iterative process portrayed by Algorithm 1, and also it is not a hard (equality) constraint. Constraint (17) as a hard constraint includes the product of two variables $V_{i,t}^{sqr}$ and $I_{ij,t}^{sqr}$, and also two squared terms, i.e., $P_{ij,t}^2$ and $Q_{ij,t}^2$. Therefore, a linearization technique based on [36] must be applied to reformulate (17). Toward this end, (17) is replaced with constraints (20)–(27), as shown hereunder. Note that in the linearization process, first $V_{i,t}^{sqr}$ is approximated with the

nominal voltage, V. Then, each square $P^2_{ij,t}$ and $Q^2_{ij,t}$ is linearized considering the parameter $m^s_{ij,y}$ and the respective variables $\Delta^p_{ij,t,y}$ and $\Delta^q_{ij,t,y}$.

$$V^2 \times I^{sqr}_{ij,t} = \sum_{y=1}^{Y} \left(m^s_{ij,y} \times \Delta^p_{ij,t,y} \right) + \sum_{y=1}^{Y} \left(m^s_{ij,y} \times \Delta^q_{ij,t,y} \right); \quad \forall ij \in \mathcal{L}, \forall t \in \mathcal{T} \tag{20}$$

$$p^+_{ij,t} - p^-_{ij,t} = P_{ij,t}; \quad \forall ij \in \mathcal{L}, \ \forall t \in \mathcal{T} \tag{21}$$

$$p^+_{ij,t} + p^-_{ij,t} = \sum_{y=1}^{Y} \Delta^p_{ij,t,y}; \ \forall ij \in \mathcal{L}, \forall t \in \mathcal{T} \tag{22}$$

$$q^+_{ij,t} - q^-_{ij,t} = Q_{ij,t}; \forall ij \in \mathcal{L}, \quad \forall t \in \mathcal{T} \tag{23}$$

$$q^+_{ij,t} + q^-_{ij,t} = \sum_{y=1}^{Y} \Delta^q_{ij,t,y}; \quad \forall ij \in \mathcal{L}, \forall t \in \mathcal{T} \tag{24}$$

$$0 \le \Delta^p_{ij,t,y} \le \bar{\Delta}^s_{ij}; \quad \forall ij \in \mathcal{L}, \ \forall t \in \mathcal{T}, \forall y = 1 \ldots Y \tag{25}$$

$$0 \le \Delta^q_{ij,t,y} \le \bar{\Delta}^s_{ij}; \quad \forall ij \in \mathcal{L}, \ \forall t \in \mathcal{T}, \forall y = 1 \ldots Y \tag{26}$$

$$0 \le p^+_{ij,t}; p^-_{ij,t}; q^+_{ij,t}; q^-_{ij,t}; \quad \forall ij \in \mathcal{L}, \ \forall t \in \mathcal{T} \tag{27}$$

Fig. 6 illustrates the linearization process related to the quadratic term $P^2_{ij,t}$. The same process is applied to linearize $Q^2_{ij,t}$.

Note that in (20), the term $P^2_{ij,t}$ is replaced with the product between parameter $m^s_{ij,y}$ and variable $\Delta^p_{ij,t,y}$. In Fig. 6, the set of points $(P_{ij,t}, P^2_{ij,t})$ determines a quadratic function whose linearization is done by intervals using lines $y = 1$, $y = 2$, $y = 3, \ldots, y =$ Y. On the horizontal axis, $P_{ij,t}$ is divided into intervals $\Delta^p_{ij,t,1}$, $\Delta^p_{ij,t,2}$, $\Delta^p_{ij,t,3}, \ldots,$ and $\Delta^p_{ij,t,y}$. Each of these variables has a maximum limit of $\bar{\Delta}^s_{ij}$, as shown in (25). Moreover, the values on the vertical axis are $1[\bar{\Delta}^s_{ij}]^2$, $4[\bar{\Delta}^s_{ij}]^2$, $9[\bar{\Delta}^s_{ij}]^2, \ldots,$ and $Y^2[\bar{\Delta}^s_{ij}]^2$. Note also that the slope related to each line y, $m^s_{ij,y}$, is obtained from the right triangles indicated by the green arrows. Thus, the slope $m^s_{ij,1}$ related to line $y = 1$ is calculated considering the sides $\Delta^p_{ij,t,1}$ (with maximum value $\bar{\Delta}^s_{ij}$) and $1[\bar{\Delta}^s_{ij}]^2$, resulting in $m^s_{ij,1} = 1[\bar{\Delta}^s_{ij}]$. For $m^s_{ij,2}$ related to $y = 2$, the calculation considers sides $4[\bar{\Delta}^s_{ij}]^2 - 1[\bar{\Delta}^s_{ij}]^2$ and $\Delta^p_{ij,t,2}$ of maximum value $\bar{\Delta}^s_{ij}$. Therefore, $m^s_{ij,2} = 3[\bar{\Delta}^s_{ij}]$. This is done similarly for the rest of the lines up to $y = Y$. In this case, $m^s_{ij,y}$ slope is calculated as $(2y - 1)[\bar{\Delta}^s_{ij}]$. Through the established equality, in the horizontal axis, such as $Y\bar{\Delta}^s_{ij} = V\bar{I}_{ij}$, the value of $\bar{\Delta}^s_{ij}$ can be calculated assuming the value of Y, and knowing the nominal voltage, V, as well as the maximum current limit, $\bar{I}_{ij}$, in each branch ij of the EG shown in Fig. 7.

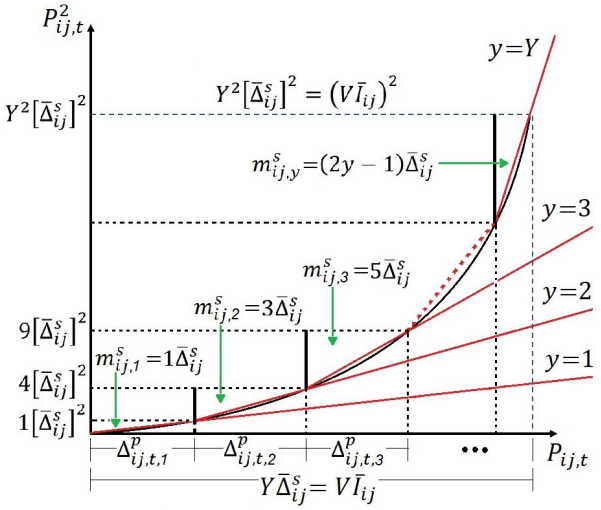

FIGURE 6. Linearization process.

IV. CASE STUDY

A. TEST SYSTEM

In this section, the case study based on the EG depicted in Fig. 7, is analyzed. The system is a radial distribution network whose load flow is calculated based on the method presented in [35]. Note that the network covers 34 nodes, in which, node 1 represents the substation ($t^b_i = 1$), nodes 3, 6, 7, and 10 represent the transfer nodes ($t^b_i = 0$), and finally, the rest of the nodes are called demand nodes ($t^b_i = 0$) [37]–[39]. Transfer nodes ($t^b_i = 0$) allow the transfer of power flow between these nodes and the adjacent nodes. For example, through node 10, power is transferred to nodes 31 and 11, which serve residential and commercial consumer units, respectively. In addition, transfer nodes are characterized such that no consumer units are connected to them. Demand nodes are differentiated by the type of consumers, such as residential units ($t^l_i = 1$) at nodes from 13 to 16, and from 26 to 34; commercial units ($t^l_i = 2$) at nodes 11, 12, and 21; and, finally, industrial units ($t^l_i = 3$) at nodes 2, 4, 5, 8, 9, also from 17 to 20, and from 22 to 24. Note that in Fig. 7 the residential, commercial, and industrial units are highlighted in red, green, and blue, respectively. The technical data for this EG are detailed in Table 3. The nominal voltage, V, in the EG is 11 kV (distribution substation). Moreover, the magnitude of voltage in the rest of the nodes i varies between a minimum, $\underline{V}$, and maximum, $\overline{V}$, value, both corresponding to 0.95 and 1.05 of the value of V. The main features of electrical equipment in each consumer unit are provided in Table 2. The proposed model is applied to a one-day time horizon, divided into 24 periods ($|T| = 24$) each of one hour ($\Delta t = 1$). Aiming to lead the shifting of the consumption time intervals of each electrical equipment, tariff signals in off-peak (00h–18h, and 23h–00h the same day), intermediate (18h and 22h), and peak (19h–21h) are considered as tabulated in Table 4 [40]. This model is implemented in AMPL [41] and solved via the commercial solver CPLEX [42]. In order to find the optimal solution to the proposed MIQCP problem, a 2.67-GHz computer with 3GB of RAM is used. The total CPU time for solving the proposed model on the test system is about 50.2 s. In addition, statistical information related to the proposed model is reported in Table 5.

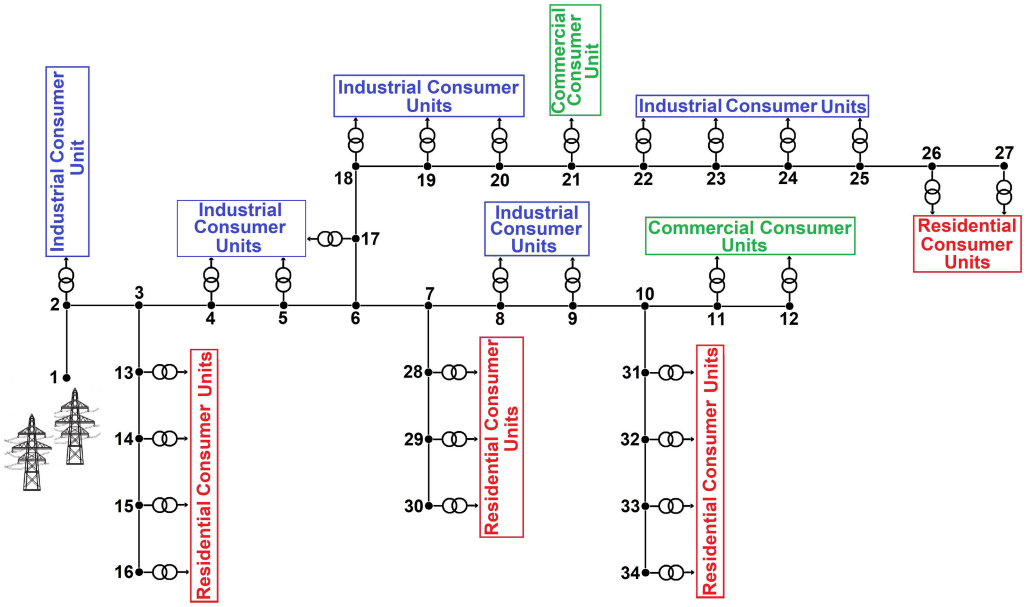

FIGURE 7. The 34-node test EG.

TABLE 3. Technical data of the 34-node EG.

i-j	z_{ij} (Ω)	$\overline{I}_{ij}$ (A)	i-j	z_{ij} (Ω)	$\overline{I}_{ij}$ (A)
1-2	1.17	1100	18-19	2.07	500
2-3	1.07	1000	19-20	1.89	500
3-4	1.64	1000	20-21	1.89	500
4-5	1.49	1000	21-22	2.62	300
5-6	1.49	1000	22-23	2.62	300
6-7	3.14	300	23-24	3.14	300
7-8	2.09	300	24-25	2.09	300
8-9	3.14	300	25-26	1.31	100
9-10	2.09	300	26-27	1.04	100
10-11	1.31	100	7-28	1.57	100
11-12	1.04	100	28-29	1.57	100
3-13	1.57	100	29-30	1.57	100
13-14	2.09	100	10-31	1.57	100
14-15	1.04	100	31-32	2.09	100
15-16	0.52	100	32-33	1.57	100
6-17	1.79	100	33-34	1.08	100
17-18	1.64	500	-	-	-

TABLE 4. Electricity price.

Hourly	Off-peak	Intermediate	Peak
Price ($/kWh)	0.22419	0.32629	0.51792

TABLE 5. Statistics of the proposed model.

Variables	Number of variables
ψ_t, ψ_t^{av}, ψ^{lp}	$2 \times \lvert\mathcal{T}\rvert + 1$
$\Pi_{i,k,t}^{conn}$, $\Pi_{i,k,t}^{dconn}$, $\Pi_{i,k,t}^{oc}$, $\Delta\Pi_{i,k,t}$	$4 \times \lvert\mathcal{B}\rvert \times \lvert\mathcal{K}\rvert \times \lvert\mathcal{T}\rvert$
$\Delta_{ij,t,y}^{p}$, $\Delta_{ij,t,y}^{q}$	$2 \times \lvert\mathcal{L}\rvert \times \lvert\mathcal{T}\rvert \times \lvert 1..Y\rvert$
$I_{ij,t}^{sqr}$, $P_{ij,t}$, $p_{ij,t}^{+}$, $p_{ij,t}^{-}$, $Q_{ij,t}$, $q_{ij,t}^{+}$, $q_{ij,t}^{-}$	$7 \times \lvert\mathcal{L}\rvert \times \lvert\mathcal{T}\rvert$
$n_{i,k,u,v}$	$\lvert\mathcal{B}\rvert \times \lvert\mathcal{K}\rvert \times \lvert\mathcal{T}\rvert^2$
$P_{i,t}^{d}$, $P_{i,t}^{s}$, $Q_{i,t}^{d}$, $Q_{i,t}^{s}$, $V_{i,t}^{sqr}$	$5 \times \lvert\mathcal{B}\rvert \times \lvert\mathcal{T}\rvert$
Total	665 257
Constraints	**Number of constraints**
(2) – (6)	$5 \times \lvert\mathcal{B}\rvert \times \lvert\mathcal{K}\rvert \times \lvert\mathcal{T}\rvert$
(7), (8) – (10), (11), (12)	$\lvert\mathcal{K}\rvert \times \lvert\mathcal{T}\rvert + 4 \times \lvert\mathcal{T}\rvert + 1$
(13) – (15), (19), (27)	$4 \times \lvert\mathcal{B}\rvert \times \lvert\mathcal{T}\rvert$
(16) – (18), (20) – (24)	$12 \times \lvert\mathcal{L}\rvert \times \lvert\mathcal{T}\rvert$
(25) – (26)	$2 \times \lvert\mathcal{L}\rvert \times \lvert\mathcal{T}\rvert \times \lvert 1..Y\rvert$
Total	143 617

B. ITERATIVE PROCESS

Algorithm 1 shows the iterative process that allows evaluating the LF of the EG presented in Fig. 7, using the proposed MIQCP model. This algorithm is run once the values of $N_{k,t}$ and $\pi_{i,k,t}^{hc}$ are known, using the MCS algorithm (shown in Fig. 2), and which in turn are the input data for the MIQCP model. At the start of the iterative process, the values Γ^0, $\overline{\Gamma}$, and e are set to zero. Afterward, the counter value e is evaluated under condition $e = 0$. In checking this condition, the MIQCP model is solved without considering constraint (12), and then, the value of Γ^0 is calculated as the maximum difference value $\left|\psi_t - \psi^{lp}\right|$. Next, after obtaining the value of Γ^0, condition $e \geq 1$ is evaluated. When this condition is met, then $\overline{\Gamma}$ is obtained as $\Gamma^0 - \alpha \times e$. Once the value of $\overline{\Gamma}$ is known, the MIQCP model is run, but this time considering constraint (12). Then, the counter value is updated using $e = e + 1$. After updating e, this value is evaluated under the condition $e = n^{iter}$. Thus, when e reaches the predefined iteration value, the iterative process ends; otherwise, the process continues to the next iteration.

Fig. 8 shows the $\overline{\Gamma}$ values obtained via the aforementioned iterative process. The initial value of $\overline{\Gamma}$ is obtained as $\Gamma^0 - \alpha e$, after the value of Γ^0 has been calculated as $Max_{\forall t \in T}\left\{\left|\psi_t - \psi^{lp}\right|\right\}$, adopting the value of 1000 kWh. Here, the value of step α is set to 10 kWh. Thus, in each iteration e, product $\alpha \times e$ reduces the value adopted by $\overline{\Gamma}$ gradually (e.g., iteration 1, 10×1; iteration 2, 10×2; …; etc.), which in turn reshapes the optimal consumption

Algorithm 1: Iterative Process for Evaluating the Proposed MIQCP Model

Start
Initialize: $\Gamma^0 \leftarrow 0$; $\overline{\Gamma} \leftarrow 0$; $e \leftarrow 0$;
do
  if $e = 0$, **then**
    Run MIQCP model without (12);
    $\Gamma^0 \leftarrow Max_{\forall t \in T} \left| \psi_t - \psi^{lp} \right|$;
  end if
  if $e \geq 1$, **then**
    $\overline{\Gamma} \leftarrow \Gamma^0 - \alpha \times e$;
    Run MIQCP model with (12);
  end if
  $e = e + 1$;
  if $e = n^{iter}$, **then**
    break;
  else
    continue;
  end if
While true
End

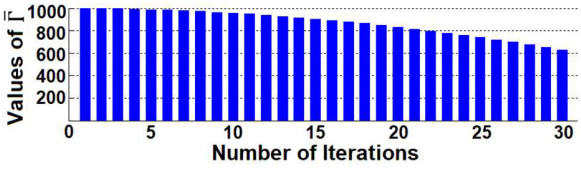

FIGURE 8. Variation of $\overline{\Gamma}$ during the execution of algorithm 1.

profile, $\Pi^{oc}_{i,k,t}$, through the ψ_t and ψ^{lp} values present in the constraint (12). It is worth mentioning that, in each iteration e, the LF evaluated considering the average consumption value, ψ^{lp}, and the maximum value of ψ_t, $\overline{\psi}_t$, for the day. Thus, once the MIQCP model has been solved in each iteration, and knowing the values of the variables mentioned above, the value of the LF is obtained as $\psi^{lp}/\overline{\psi}$. The behavior related to the values of the LF, obtained via the iterative process, is depicted in Fig. 9. It can be seen in both Figs. 8 and 9 that the predefined number of iterations n^{iter}, is equal to 30. This value was established based on performing several tests. During the evaluation of the proposed model, it has been observed that the CPLEX *solver* ends the execution automatically, always after 30 iterations, considering the values of α and Γ^0 mentioned above. Therefore, in this first approach to this problem, n^{iter} equal to 30 is assumed. For this number of iterations, $\overline{\Gamma}$ decreases (Fig. 8) while LF oscillates (Fig. 9). During the iterative process, LF adopts values of 0.58 and 0.73 for certain values of e. Furthermore, after 23 iterations, the LF value remains constant at 0.73. Because this last value is close to 1, the optimal consumption profile, $\pi^{oc}_{i,k,t}$, for the electricity grid shows a reduction in energy costs for all consumers, especially during peak consumption periods. It is worth mentioning that the gradual reduction of $\overline{\Gamma}$ during the

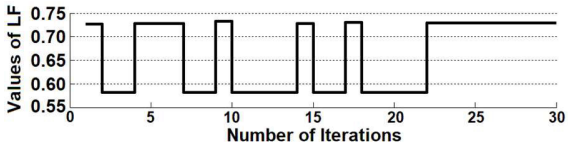

FIGURE 9. Variation of the LF during the execution of algorithm 1.

iterative process does not directly influence the LF values. To better analyze this fact, future research will be addressed considering the linearized form of the constraint (12), since this constraint is part of the objective function.

C. DISCUSSION OF RESULTS

Figs. 10(a), (b), and (c) show the profiles of habitual and optimal consumption, in blue and red lines, respectively, for each type of consumer unit. Fig. 10(a) shows both profiles for the total of residential consumption units. It is observed that within the intermediate and peak periods, there is a reduction in consumption. Being that this reduction presents in the optimal profile represents 80% of the habitual consumption within that same time. In addition, the scheduling of electrical equipment, of this type of consumers, for off-peak hours shows the appearance of new consumption peaks. Likewise, the presence of new consumption peaks in the optimal profile related to the total number of commercial consumers is observed in Fig. 10(b). This consumption profile also shows a reduction in consumption, during peak hours, with a shift in consumption to periods with low energy prices. Moreover, in the peak and intermediate periods, the reduced energy reached a value of 90%. Another reduction is obtained during the morning period, that is, between hours 05h–07h. In these consumer units, energy savings are obtained by the hourly change of the production of a given product (e.g., bread, shoes, and clothes, to name just three). In Fig. 10(c), the optimal profile of industrial consumers also shows a reduction in consumption, during the peak period, in relation to their habitual profile. Note that the industrial profile is differentiated compared with residential and commercial consumers because the industrial electrical equipment has more number of effective hours of usage during the day. Therefore, the optimal profile of industrial consumers shows a reduction of consumption around 77% during hours 16h–21h, due to the shifting of the equipment that is being used for the longer-term task. In this connection, it is necessary to note that part of the reduction of energy consumption in peak and intermediate periods is shifted to hours 09h–16h and also hours 00h–05h, showing that by adopting the DSM strategies, a reduction in industry expenses in the aforementioned periods is feasible. It is worth noting that the financial gain obtained from scheduling industrial equipment within these hours is more significant for steel and petrochemical industries, as well as glass and cellulose producers, whose processes should not be interrupted. Note also how scheduling the industrial consumption during off-peak

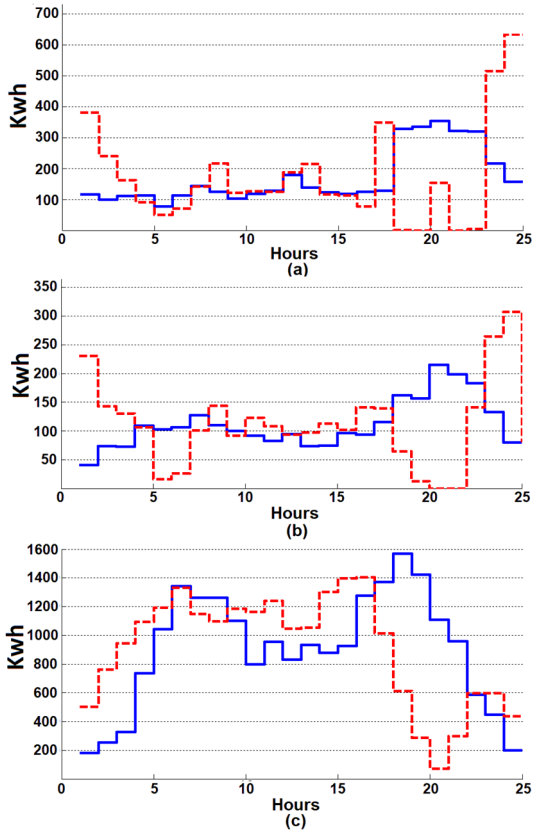

FIGURE 10. **Consumption profile of (a) residential, (b) commercial, and (c) industrial customers.**

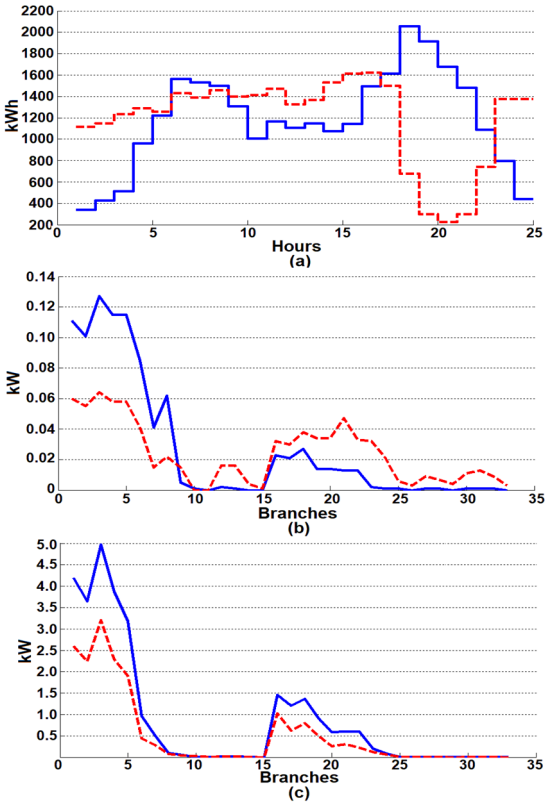

FIGURE 11. **The consumption profile of all customers (a), and active losses in periods of minimum and maximum consumption, (b) and (c).**

hours is complementary to energy consumption related to the rest of residential and commercial consumers. In other words, the DSM strategy that considers the improvement of the LF, for EG, performs the efficient scheduling of the different types of equipment, so that the residential, commercial, and industrial consumption profiles can be integrated and thus the optimal profile related to the total number of these consumers, see Fig. 11(a), do not show new consumption peaks (greater than the habitual peak) within the hours with the lowest energy cost, which guarantees an increase in the value of the LF for the entire EG.

Fig. 11(a) depicts the profile of habitual ($\pi^{hc}_{i,k,t}$ in blue) and optimal ($\Pi^{oc}_{i,k,t}$ in red) consumption. As previously mentioned, the LF of the optimal profile (0.73) was improved, compared to the habitual profile (0.58). This fact is evident since consumption within peak hours has been shifted to off-peak hours without the formation of new peaks that could compromise the performance of EG. Note that the habitual profile shows higher consumption in the intermediate and peak periods due to the strong influence of industrial consumers on the total of units. Moreover, the distribution of habitual consumption values (in blue line) is heterogeneous, with peaks and valleys corresponding to the low LF value. By applying the proposed model, the optimal profile increases the LF value. For this value, this profile presents a more homogeneous distribution during the day, specifically during off-peak periods, guaranteeing the efficient use of energy consumption during the day, thus demonstrating the potential of the DSM strategies to meet the operational requirements of the EG.

Figs. 11(b) and (c) show the losses of active power in the EG, for both habitual and optimal consumption profiles, for the corresponding periods of minimum and maximum consumption. For both figures, on the horizontal axis, the branches are enumerated considering the order shown in Table 6. Following this order, in Fig. 11(b), related to the corresponding periods of minimum consumption, it can be seen that the branches located close to the substation (e.g., whose order is 1, 2, 3, 4, …, 9) show a reduction in losses of active power for the optimal profile (red line) compared to the habitual profile (blue line). Moreover, an increase in active power losses occurs in the branches associated with nodes 15 and 25 (e.g., with order 16, 17, 18, …, 24) with a higher presence of industrial consumers. Fig. 11(c) depicts active losses, in the corresponding periods of maximum consumption, that is, for the habitual profile (blue line) in the 18h period, and for the optimal (red line) profile in the 16h period. Note that the active losses in the EG branches, which correspond to the optimal profile, are less than or equal to the active losses related to the habitual profile. Note also that the branches organized in the order 10 to 15, and 25 to 33, present active power losses close to zero, with the majority of nodes belonging to residential units. To conclude, Table 7 shows

TABLE 6. Ordinal arrangement of branches in the 34-node test system.

n°	1	2	3	4	5
i-j	1-2	2-3	3-4	4-5	5-6
n°	6	7	8	9	10
i-j	6-7	7-8	8-9	9-10	10-11
n°	11	12	13	14	15
i-j	11-12	3-13	13-14	14-15	15-16
n°	16	17	18	19	20
i-j	6-17	17-18	18-19	19-20	20-21
n°	21	22	23	24	25
i-j	21-22	22-23	23-24	24-25	25-26
n°	26	27	28	29	30
i-j	26-27	7-28	28-29	29-30	10-31
n°	31	32	33	-	-
i-j	31-32	32-33	33-34	-	-

TABLE 7. Costs of energy consumption related to types of consumers.

Total consumer units	Total Costs (10^3\$)		Variation in costs (%)
	Habitual Profile	Optimal Profile	
Residential	1.220	0.998	18.19
Commercial	0.961	0.780	18.83
Industrial	6.223	5.170	16.92
Total number of units	8.404	6.948	17.33

the total costs per energy consumption for each consumer class (i.e., residential, commercial, and industrial) and also for all the consumers. The total costs (10^3\$) are presented for both habitual and optimal consumption profiles. For each residential, commercial, and industrial class, the optimal consumption profile obtained by the proposed MIQCP model shows a considerable reduction, i.e., 18.19%, 18.83%, and 16.92% compared to their respective habitual consumption profile, respectively. In the case of the total number consumer units, the reduction in the cost of consumed energy represents 17.33%. This fact reveals the energy savings that can be achieved in each consumer class as well as for the total number of customer served by the energy distribution company, once they are participants in a DSM program. As a consequence of this reduction in energy consumption costs, especially during periods of higher energy tariff, the energy company avoids unnecessary expenses in purchasing energy.

V. CONCLUSION

In this paper, a methodology for assessing the LF of a modified 34-node EG with different types of consumers has been proposed. In the methodology, a MIQCP model has been introduced within an iterative process aiming to find the best value of the LF through a DSM strategy, while the total costs associated with purchasing energy by the electricity company are minimized. Furthermore, an MCS algorithm has been implemented in order to simulate the habitual consumption patterns in residential, commercial, and industrial consumer classes. In addition, a tariff structure based on three levels (peak, intermediate, and off-peak) has been utilized to efficiently schedule the periods of consumption of electrical equipment for the day ahead. The obtained results show that the application of DSM strategies to enhance the performance of an EG, i.e., the best value of LF, allows achieving striking amounts of savings for energy companies. This is due to the reduction in the purchase of energy in time intervals of peak demand. Moreover, the reduction in consumption during peak periods, without the occurrence of new peaks in other periods, allows to relieve congestion in the main feeder as well as reducing fatigue in assets, specifically in the power transformer. Consequently, a significant reduction in active energy losses is also achieved, which corroborates the effectiveness of the proposed methodology as a tool for analyzing and evaluating DSM strategies by the electricity company, as well as by the system aggregator.

Although the proposed MIQCP model has provided preliminary results, especially when it comes to increasing the LF, there are aspects within the methodology that need to be improved, among the main ones we can mention: i) In addition to the linearization of the constraint (17) it is necessary to consider the linearization of the constraint (12) in order to guarantee a space of convex solutions; ii) the iterative process, i.e., Algorithm 1, when the constraint (12) is considered in the objective function; and iii) different amount of equipment for each residential, commercial, and industrial consumer unit. It is worth mentioning that, currently, this last aspect is being improved considering the level of complexity involved in the resolution of the MIQCP model, as well as the influence on the LF values to be obtained.

REFERENCES

[1] J. Ekanayake, K. Liyanage, J. Wu, A. Yokoyama, and N. Jenkins, *Smart Grid Technology and Applications*. Hoboken, NJ, USA: Wiley, 2012.

[2] A. B. M. Shawkat Ali, *Smart Grid Opportunities, Development Trends*. London, U.K.: Springer-Verlag, 2013.

[3] P. Balakrishna, K. Rajagopal, and K. S. Swarup, "Distribution automation analysis based on extended load data from AMI systems integration," *Int. J. Elect. Power Energy Syst.*, vol. 86, pp. 154–162, Mar. 2017.

[4] H. Shareef, M. S. Ahmed, A. Mohamed, and E. Al Hassan, "Review on home energy management system considering demand responses, smart technologies, and intelligent controllers," *IEEE Access*, vol. 6, pp. 24 498–24 509, Apr. 2018.

[5] J. Garcia-Villalobos, I. Zamora, P. Eguia, E. Torres, A. Etxegarai, and J. I. San Martin, "Optimization of load factor in distribution networks with high share of plug-in electric vehicles and photovoltaic generation," in *Proc. 52nd Int. Universities Power Eng. Conf. (UPEC)*, Aug. 2017, pp. 1–6.

[6] J. Surai and V. Surapatana, "Load factor improvement in industrial sector using load duration curves," in *Proc. Int. Elect. Eng. Congr.*, 2014, pp. 1–4.

[7] K. Trongwanichnam, S. Thitapars, and N. Leeprechanon, "Impact of plug-in electric vehicles load planning to load factor and total generation cost in a power system," in *Proc. IEEE PES GTD Grand Int. Conf. Expo.*, Mar. 2019, pp. 599–604.

[8] A. Jabbarzadeh, B. Fahimnia, and S. Rastegar, "Green and resilient design of electricity supply chain networks: A multiobjective robust optimization approach," *IEEE Trans. Eng. Manag.*, vol. 66, no. 1, pp. 52–72, Feb. 2019.

[9] R. Faranda and H. Hafezi, "Reassessment of voltage variation for load power and energy demand management," *Int. J. Elect. Power Energy Syst.*, vol. 106, pp. 320–326, Mar. 2019.

[10] K. Pramelakumari, S. R. Anand, V. P. J. Raj, and E. A. Jasmin, "Short-term load forecast of a low load factor power system for optimization of merit order dispatch using adaptive learning algorithm," in *Proc. Int. Conf. Power, Signals, Controls Comput.*, Jan. 2012, pp. 1–7.

[11] R. F. Chang and C. N. Lu, "Feeder reconfiguration for load factor improvement," in *Proc. IEEE Power Eng. Soc. Winter Meeting. Conf. Process.*, May 2012, pp. 980–984.
[12] J. Li, C. Yuan, Z. Zheng, and F. Li, "Load factor based transmission network pricing: An evaluation for the improved ICRP method," in *Proc. 48th Int. Universities' Power Eng. Conf. (UPEC)*, Sep. 2013, pp. 1–6.
[13] P. J. Douglass, R. G. Valle, J. Ostergaard, and O. C. Tudora, "Voltage-sensitive load controllers for voltage regulation and increased load factor in distribution systems," *IEEE Trans. Smart Grid*, vol. 5, no. 5, pp. 2394–2401, Sep. 2014.
[14] B. J. Saikia, M. Manas, and D. C. Baruah, "Distribution loss reduction in a university of north east india through load factor improvement," in *Proc. Int. Conf. Energy Syst. Appl.*, Oct. 2015, pp. 203–208.
[15] A. Dogan, M. Kuzlu, M. Pipattanasomporn, S. Rahman, and T. Yalcinoz, "Impact of EV charging strategies on peak demand reduction and load factor improvement," in *Proc. 9th Int. Conf. Elect. Electron. Eng. (ELECO)*, Nov. 2015, pp. 374–378.
[16] Z. Ren *et al.*, "Distributed power flow considering network loss allocation and load factor of subareas," in *Proc. 35th Chin. Control Conf. (CCC)*, Jul. 2016, pp. 2820–2824.
[17] A. S. Al Fardan, K. S. Al Gahtani, and M. Asif, "Demand side management solution through new tariff structure to minimize excessive load growth and improve system load factor by improving commercial buildings energy performance in saudi arabia," in *Proc. IEEE Int. Conf. Smart Energy Grid Eng. (SEGE)*, Aug. 2017, pp. 308–320.
[18] W.-Y. Chiu, J.-T. Hsieh, and C.-M. Chen, "Pareto optimal demand response based on energy costs and load factor in smart grid," *IEEE Trans. Ind. Informat.*, vol. 16, no. 3, pp. 1811–1822, Mar. 2020.
[19] K. Margellos and S. Oren, "Capacity controlled demand side management: A stochastic pricing analysis," *IEEE Trans. Power Syst.*, vol. 31, no. 1, pp. 706–717, Jan. 2016.
[20] A. C. Chapman, G. Verbic, and D. J. Hill, "Algorithmic and strategic aspects to integrating demand-side aggregation and energy management methods," *IEEE Trans. Smart Grid*, vol. 7, no. 6, pp. 2748–2760, Nov. 2016.
[21] B. Lokeshgupta and S. Sivasubramani, "Multi-objective dynamic economic and emission dispatch with demand side management," *Int. J. Elect. Power Energy Syst.*, vol. 97, pp. 334–343, Apr. 2018.
[22] H. Yang, Y. Zhang, Y. Ma, M. Zhou, and X. Yang, "Reliability evaluation of power systems in the presence of energy storage system as demand management resource," *Int. J. Elect. Power Energy Syst.*, vol. 110, pp. 1–10, Sep. 2019.
[23] Z. Ding, P. Sarikprueck, and W.-J. Lee, "Medium-term operation for an industrial customer considering demand-side management and risk management," *IEEE Trans. Ind. Appl.*, vol. 52, no. 2, pp. 1127–1135, Apr. 2016.
[24] X. Tang and J. V. Milanović, "Assessment of the impact of demand-side management on distribution network voltage stability," *CIRED-Open Access Proc. J.*, vol. 2017, no. 1, pp. 2118–2121, Oct. 2017.
[25] K. Wang, H. Li, S. Maharjan, Y. Zhang, and S. Guo, "Green energy scheduling for demand side management in the smart grid," *IEEE Trans. Green Commun. Netw.*, vol. 2, no. 2, pp. 596–611, Jun. 2018.
[26] C. P. Mediwaththe, E. R. Stephens, D. B. Smith, and A. Mahanti, "Competitive energy trading framework for demand-side management in neighborhood area networks," *IEEE Trans. Smart Grid*, vol. 9, no. 5, pp. 4313–4322, Sep. 2018.
[27] X. Yang, Y. Zhang, H. He, S. Ren, and G. Weng, "Real-time demand side management for a microgrid considering uncertainties," *IEEE Trans. Smart Grid*, vol. 10, no. 3, pp. 3401–3414, May 2019.
[28] P. C. Robert, *Monte Carlo Statistical Methods*. New York, NY, USA: Springer, 2004.
[29] T. Logenthiran, D. Srinivasan, and T. Z. Shun, "Demand side management in smart grid using heuristic optimization," *IEEE Trans. Smart Grid*, vol. 3, no. 3, pp. 1244–1252, Sep. 2012.
[30] A. Talwariya, P. Singh, and M. Kolhe, "A stepwise power tariff model with game theory based on monte-carlo simulation and its applications for household, agricultural, commercial and industrial consumers," *Int. J. Elect. Power Energy Syst.*, vol. 111, pp. 14–24, Oct. 2019.
[31] J. A. Jardini, C. M. V. Tahan, M. R. Gouvea, S. U. Ahn, and F. M. Figueiredo, "Daily load profiles for residential, commercial and industrial low voltage consumers," *IEEE Trans. Power Del.*, vol. 15, no. 1, pp. 375–380, Jan. 2000.
[32] L. Chuan and A. Ukil, "Modeling and validation of electrical load profiling in residential building in Singapore," *IEEE Trans. Power Syst.*, vol. 30, no. 5, pp. 2800–2809, Sep. 2015.
[33] E. Zio, M. Delfanti, L. Giorgi, V. Olivieri, and G. Sansavini, "Monte Carlo simulation-based probabilistic assessment of DG penetration in medium voltage distribution networks," *Int. J. Elect. Power Energy Syst.*, vol. 64, pp. 852–860, Jan. 2015.
[34] Y. Wang and D. Infield, "Markov chain Monte Carlo simulation of electric vehicle use for network integration studies," *Int. J. Elect. Power Energy Syst.*, vol. 99, pp. 85–94, Jul. 2018.
[35] R. G. Cespedes, "New method for the analysis of distribution networks," *IEEE Trans. Power Del.*, vol. 5, no. 1, pp. 391–396, Jan. 1990.
[36] L. H. Macedo, J. F. Franco, M. J. Rider, and R. Romero, "Optimal operation of distribution networks considering energy storage devices," *IEEE Trans. Smart Grid*, vol. 6, no. 6, pp. 2825–2836, Apr. 2015.
[37] H. B. Funmilayo, J. A. Silva, and K. L. Butler-Purry, "Overcurrent protection for the IEEE 34-node radial test feeder," *IEEE Trans. Power Del.*, vol. 27, no. 2, pp. 459–468, Apr. 2012.
[38] J. A. Silva, H. B. Funmilayo, and K. L. Bulter-Purry, "Impact of distributed generation on the IEEE 34 node radial test feeder with overcurrent protection," in *Proc. 39th North Amer. Power Symp.*, Sep. 2007, pp. 49–57.
[39] N. Mwakabuta and A. Sekar, "Comparative study of the IEEE 34 node test feeder under practical simplifications," in *Proc. 39th North Amer. Power Symp.*, Sep. 2007, pp. 484–491.
[40] National Electric Energy Agency (ANEEL). *Normative Resolution 733-White Tariff*. Accessed: Jul. 14, 2021. [Online]. Available: https://www.aneel.gov.br/tarifa-branca
[41] R. Fourer, D. M. Gay, B. W. Kernighan, *AMPL: A Modeling Language for Mathematical Programming*. Pacific Grove, CA, USA: Brooks/Cole-Thomson Learning, 2003.
[42] *IBM ILOG CPLEX V 12.1, User's Manual for CPLEX*, CPLEX Division, Incline Village, NV, USA, 2009.

FERNANDO V. CERNA (Member, IEEE) received the B.Sc. degree in electrical engineering from the National University of Callao (UNAC), Lima, Peru, in 2008, and the M.Sc. and Ph.D. degrees in electrical engineering from São Paulo State University (UNESP), Ilha Solteira, Brazil, in 2013 and 2017, respectively. From 2017 to 2019, he was a Post-Doctoral Fellow with the State University of Londrina (UEL), Paraná, Brazil. He is currently an Assistant Professor with the Department of Electrical Engineering, Center for Science and Technology, Federal University of Roraima (UFRR), Roraima, Brazil. Moreover, he is the Leader of the Research Group Smart Management of Electric Power Systems Certified by the National Council for Scientific and Technological Development (CNPq). His research interests include efficient energy management of electricity distribution networks, microgrids, energy communities, sustainable cities, and electromobility.

MAHDI POURAKBARI-KASMAEI (Senior Member, IEEE) received the Ph.D. degree in electrical engineering, power systems from São Paulo State University (UNESP), Ilha Solteira, Brazil, in 2015. He was a Post-Doctoral Fellow with UNESP and a Visiting Researcher with the University of Castilla-La Mancha, Spain. He was a project executive or a principal investigator of several practical and academic projects and also a consultant in an electric power distribution company. He is currently an Assistant Professor with the Department of Electrical Engineering and Automation, Aalto University, Finland, where he used to be a Post-Doctoral Researcher for more than three years. His research interests include power systems planning, operations, economics, and environmental issues, and power system protection and transients. He is the Chairman of the IEEE PES Finland IE13/PE31/34/PEL35 Joint Chapter, an Ambassador of Clean Energy in the IEEE Finland Section, the General Chair of IEEE PES ISGT-Europe 2021 Conference, and an Associate Editor of several journals, such as IEEE Access and *Journal of Control, Automation and Electrical Systems*.

EHSAN NADERI (Graduate Student Member, IEEE) is currently pursuing the Ph.D. degree with the School of Electrical, Computer, and Biomedical Engineering, Southern Illinois University, Carbondale, IL, USA. His current research focuses on modern power systems operation and planning, in general renewable energy resources, in particular on the application of optimization techniques for enhancing smart grids security. He is also serving as an active reviewer for top-field journals.

MATTI LEHTONEN received the master's and Licentiate degrees in electrical engineering from the Helsinki University of Technology in 1984 and 1989, respectively, and the Doctor of Technology degree from the Tampere University of Technology in 1992. He was with VTT Energy, Espoo, Finland, from 1987 to 2003. Since 1999, has been a Professor with the Helsinki University of Technology (currently Aalto University), where he is also the Head of power systems and high voltage engineering. His main activities include power system planning and asset management, power system protection, including earth fault problems, harmonic related issues, and applications of information technology in distribution systems.

JAVIER CONTRERAS (Fellow, IEEE) received the B.S. degree in electrical engineering from the University of Zaragoza, Zaragoza, Spain, in 1989, the M.Sc. degree from the University of Southern California, Los Angeles, CA, USA, in 1992, and the Ph.D. degree from the University of California at Berkeley, Berkeley, CA, USA, in 1997. He is currently a Professor with the Universidad de Castilla-LaMancha, Ciudad Real, Spain. His research interests include power systems planning, operation, economics, and electricity markets.